TOMOGRAPHY AND LOCATION PROBLEMS IN CHINA USING REGIONAL TRAVEL-TIME DATA

Thomas M. Hearn and James F. Ni

New Mexico State University, Physics Department

Sponsored by Defense Threat Reduction Agency

Contract No. DTRA01-99-C-0016

ABSTRACT

Phase data from the Annual Bulletin of Chinese Earthquakes (ABCE) are being collected and used for tomographic inversion and event location problems within China. So far, we have seven years of data in computer form and six more in catalog form. Current efforts focus on regional tomography of China, comparing locations between the ABCE and other earthquake catalogs, and developing station corrections for International Monitoring System (IMS) stations in and around China.

We used the Pn phase data from the ABCE catalog to image the uppermost mantle velocity and anisotropy structure beneath China. Raypaths cover most of central and eastern China; coverage in western China and Tibet is poor. The data quality is exceptional, with Pn phases routinely identified and picked for distances from 1.5 to 9 degrees. Over 25,000 arrivals have been used in the Pn tomography algorithm. The average uppermost mantle velocity beneath China is 8.0 km/s. The Tarim, Junggar, Tsidam, and Sichaun basins have the highest Pn velocities (over 8.2 km/s). These places are cratonic terrains that were accreted to southern Asia before the Indian-Asian collision. The high velocities imply higher density mantle that may have aided in the development of these basins. The eastern Tien Shan has normal Pn velocities of 8.0 to 8.1 km/s. Pn velocity beneath Tibet decreases from south to north as previous studies have also found. Late station delays in and around Tibet attest to its 70-km thick crust. Along the southeastern Tibet margin, low Pn velocities are found, suggesting that high temperatures and possible partial melt exist in the uppermost mantle there. A region of high anisotropy surrounds Tibet. Eastern China has lower Pn velocities and thinner crust as a result of Cenozoic extension of eastern China. A very low Pn velocity (<7.7 km/s) is found north of Hainan Island. This feature may be related to the opening of the South China Sea.

We made regional travel-time plots for the ten CDSN stations in China. Two of these stations, BJI and HLR, are now IMS stations. Thus, these travel-time curves can be used for event location. Average Pg, Pn, Sg, and Sn velocities beneath these Chinese stations are 6.1 km/s, 8.0 km/s, 3.5 km/s, and 4.5 km/s respectively.

KEY WORDS: China, tomography, Pn

OBJECTIVE

New Mexico State University seismologists, in conjunction with seismologists from the Institute of Geophysics of the China Seismological Bureau (IG/CSB), have collected seismic data to calibrate IMS stations in China and to document regional phase propagation characteristics in China. We are approaching these problems through regional tomography, characterization of regional wave propagation, station calibration, and an analysis of current location capabilities in China (Figure 1).

RESEARCH ACCOMPLISHED

Data collection

Our data set of the Annual Bulletin of Chinese Earthquakes (ABCE) consists of both paper catalogs and digital data sets provided by our colleagues from the China Seismological Bureau (CSB). Paper catalogs spanning 1983 to 1995; 1991 to 1995 were also given to us in digital form. The 1986 through 1990 catalogs were typed into the computer, and work on earlier catalogs is proceeding. The data quality from the ABCE is exceptional, with Pn phases routinely identified and picked for distances of up to 9 degrees (Figure 2). Pn arrivals form the linear first-arrival portion of the travel-time curve between distances of 200 to past 1500 km.

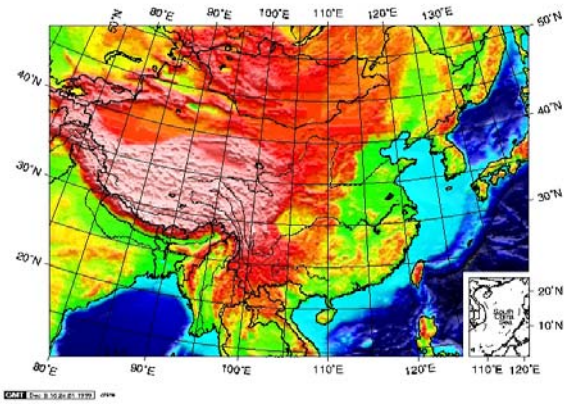

Figure 1. Shaded topography of China.

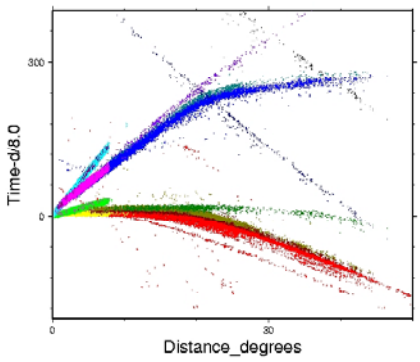

Figure 2. P-wave first arrival travel times from the Chinese bulletins (ABCE) for 1991 through 1995. Pg, Pn and a distant P branch are clearly visible. The ABCE routinely identifies arrivals as Pg, Pn, P, PP, pP, Sg, Sn, S, SS, sS, sP, PcP, S11, ScS, P11, ScP, PcS.

Station-Specific Travel Times

We have prepared travel-time curves for the CDSN stations in China (Figure 3). The two IMS stations in China, BJT and HIA, were not in existence when these data were collected; however, they replaced two nearby stations, BJI and HLR. We determined Pg, Pn, Sg, and Sn velocities for each of these stations via straight line fits. The ABCE identifies these phases to distances to 9 degrees.

Pn velocities vary from 7.9 to 8.1 km/s and Sn velocities are always 4.5 km/s. The lack of variation in Pn and Sn velocities is due to the large geographical averaging over a circle of 9 degrees radius (254 square-degrees). Pg velocities vary from 6.0 to 6.3km/s; Sg velocities vary fare 3.5-3.7 km/s. Higher Pg velocities are at Lhasa and Urumqi, both regions of thicker crust. A table of these velocities for different stations is shown below.

Table 1. Intercepts and apparent velocities for Pg, Pn, Sg, and Sn phases at CDSN stations

Station	Location	Pg	Pn	Sg	Sn
BJI	Baijiatuan	-1.1s, 6.14km/s	4.99s, 7.91km/s	-0.56s, 3.66km/s	10.26s, 4.52km/s
ENS	Enshi	0.8, 6.17	8.6, 8.13	0.5, 3.54	11.1, 4.52
HLR	Hailar	-0.2, 6.06	6.9, 8.06	-0.4, 3.52	10.1, 4.51
KMI	Kunming	0.1, 6.17	7.0, 7.94	0.7, 3.58	10.9 4.45
LSA	Lhasa	0.3, 6.28	8.4, 8.02	0.4, 3.55	13.5, 4.52
LZH	Lanzhou	-1.1, 6.07	8.0, 8.00	-1.6, 3.53	12.7, 4.55
MDJ	Mudanjiang	-0.6, 6.09	6.28, 8.01	-1.9, 3.52	9.9, 4.5
QIZ	Qiongzhong	too little data			
SSE	Shanghai	-0.6, 6.09	poor data	-1.4, 3.53	9.1, 4.47
WMQ	Urumqi	0.7, 6.29	8.5, 8.08	0.7, 3.57	13.3, 4.55

numbers refer to intercept - velocity pairs in seconds and km/s

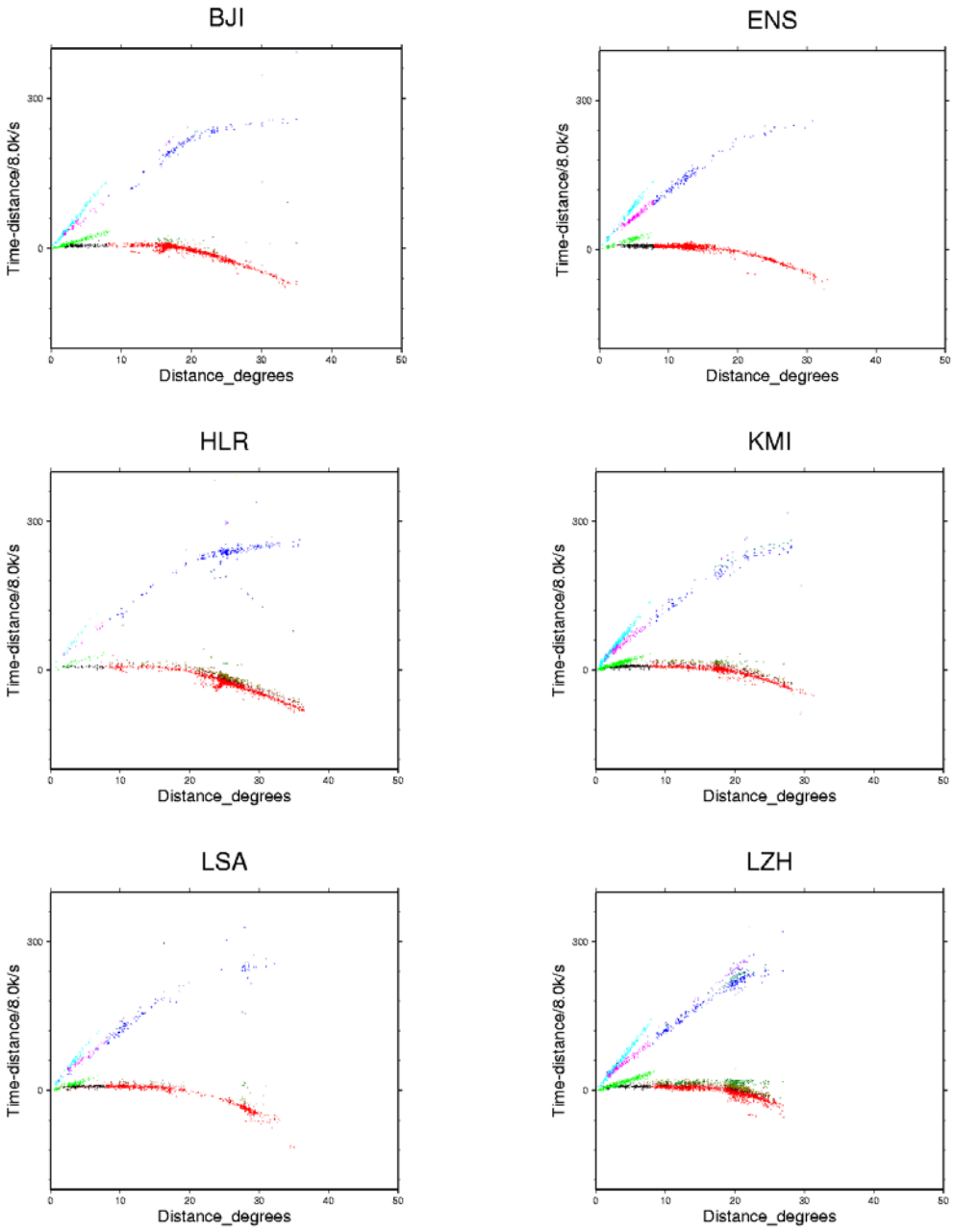
BJI
ENS
HLR
KMI
LSA
LZH
Time-distance/8.0k/s
Distance_degrees
300
0
10
20
30
40
50

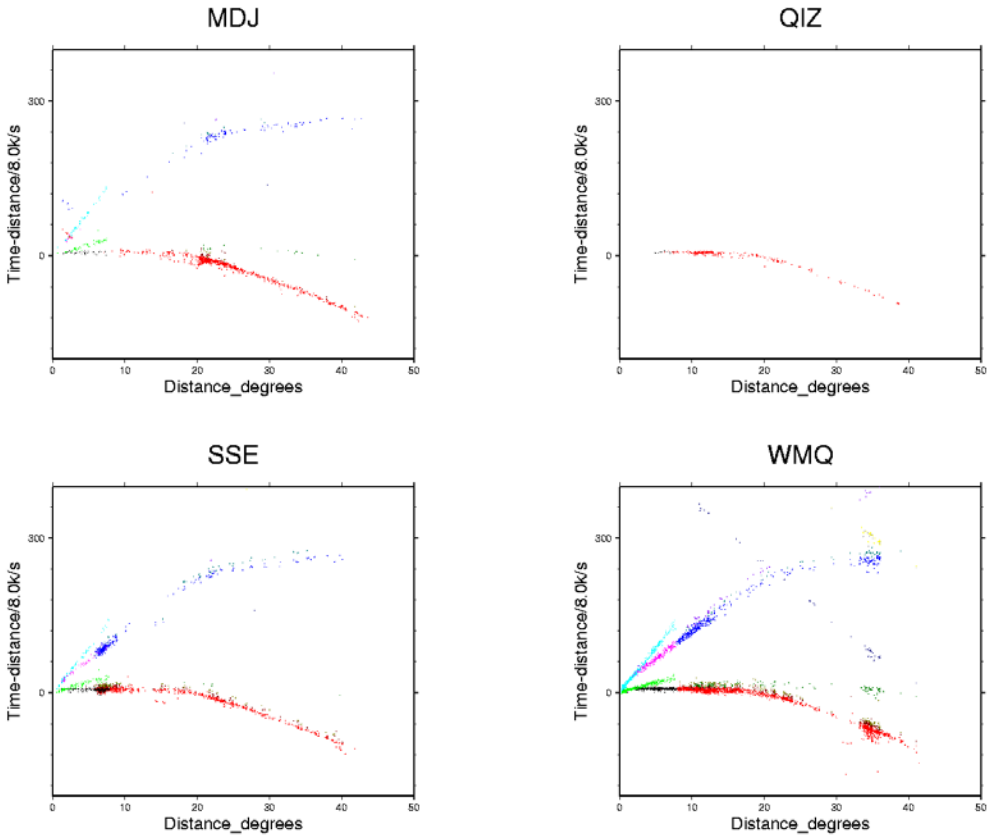

Figure 3. Reduced travel-time plots for CDSN stations. Stations BJI and HLR are next to IMS stations BJT and HIA.

Pn Tomography Beneath China

We have applied the Pn tomography algorithm of Hearn (1999) to Pn data from the ABCE to image the P-wave velocity and anisotropy at the surface of the mantle. Raypaths for these data cover most of central and eastern China; coverage in western China and Tibet is poorer, but we are now beginning to include data from other sources to remedy this. We used raypaths between 1.8 and 15 degrees distance and only stations and events with more than 9 arrivals at them. The final Pn data contains over 40,000 arrivals that span most of China (Figure 4).

The tomography algorithm has been modified to minimize the Akaike Information Criteria (AIC) as a norm (Akaike, 1973; McQuarrie and Tsai, 1998). From a practical viewpoint, the AIC is used to determine the damping constants in a damped least-squares inversion. We use it to determine the appropriate levels of the velocity and anisotropy variations in the seismic tomography. From a theoretical viewpoint, however, the AIC determines a solution that has optimal prediction capability. Thus, in seismic tomography, it will produce the best model for event location.

The inversion yields an average Pn velocity of 8.05 km/s for all of China. Figure 4 shows the regionally varying Pn velocities and anisotropy from the inversion. On Figure 5 the Pn velocity variations are superimposed upon shaded topography to demonstrate the correlation between them. The high Pn velocity regions are stable cratonic areas – Junggar Basin, Tarim Basin, Taidam Basin and Sichuan Basin. These cratonic areas were not greatly affected by tectonic and magmatic activity since their formation and hence there is lower temperature in the mantle lid and higher Pn velocity. These shield regions must also be regions of strong lithosphere. Their higher density mantle may have aided in the development of these basins. Pn velocity beneath Tibet decreases from south to north as has been found in previous Tibet studies (McNamara, 1997). This suggests that the subducted Indian plate ends somewhere beneath central Tibet. Eastern China has much lower Pn velocities. Along the southeastern Tibet margin, low Pn velocities are found suggesting that high temperatures and possible partial melt exists in the mantle there. Anisotropy is shown in Figure 4 by short line segments oriented along the fast anisotropy direction. Major regions of anisotropy are beneath the eastern Himalayan syntaxis, Sichuan Basin and Taiwan. Our resolution in the velocity and anisotropy is between two and three degrees. Because anisotropy can vary on shorter distance scales, much of it remains unresolved.

Both station and event delays represent the combined effect of crustal velocity and thickness (Figures 6 - 8). Event delays, however, are also susceptible to errors in origin time or depth in the event location. In most Pn tomography studies (e.g. Hearn, 1999), these errors create such scatter in the event delays that they are of little use. This is not the case for the ABCE data, and it indicates that events in China are exceptionally well located.

The station delays can be interpreted as a rough map of crustal thickness in China. For a constant velocity crust, 1 second of delay time represents approximately 10 km of crustal thickening. Late station and event delays in Tibet then imply that the crust there is 30 to 40 km thicker than the crust in eastern China. Events north of the Tarim Basin and in the Tien Shan also show late delays indicating crust that is 10 to 20 km thicker than eastern China. A thin crust is also apparent southeast of Tibet where extension is occurring.

Variation in Pn velocity within the Tibetan Plateau has been observed. Southern Tibet has a high Pn velocity and is probably underlain by the under-thrusting Indian continental lithosphere (Barazangi and Ni, 1983; Ni and Barazangi, 1984; Beghoul et al., 1993; Nelson et al., 1996; Huang et al., 2000). Our data in Tibet, with limited ray coverage, barely resolve the Pn velocity between northern and southern Tibet. In northern Tibet, the Pn velocity is about 7.9 km/s (also see McNamara et al., 1997). The relatively low velocity in northern Tibet has been interpreted as thermally weakened Asian mantle lid that is being squeezed between the advancing Indian lithosphere to the south and similarly rigid Tsaidam and Tarim lithosphere to the north and west (Huang et al., 2000). Unresolved is the issue of what ultimately caused the heating, and consequent weakening, of the upper mantle beneath northern Tibet. Convective removal of part of the mantle lid or prior subduction of water-rich mineral into the upper mantle leading to weakening and subsequent station heating (e.g. Yin and Harrison, 2000, Huang et al., 2000) are possibilities. In regions adjacent to the southeastern edge of the Tibetan plateau where coverage is good, we found low Pn velocity (<7.8 km/s) regions. These regions correspond to magmatic (extensive Quaternary basalt) and tectonic activity in the Panxi rift and Xiaojiang fault system. The tendency of NNE alignment of the Panxi rift suggests an orientation controlled by the simple shearing motion in the Asian lithosphere. Such an interpretation is consistent with the observation that the Panxi rift and Xiaojiang pull-apart lie in a trans-extensional tectonic environment produced by the sharing between India and Asia plate, which is currently taking place on a transform boundary along the right-lateral Sagaing fault (Guzmann-Spazelie and Ni, 1993).

Eastern China comprises the Archean North China block and South China block. These cratonic blocks collided first during the late Permian. After the collision, it experienced widespread tectono-thermal reactivation events during Late Mesozoic and Cenozoic, as indicated by emplacement of voluminous late Mesozoic granites and extensive Cenozoic volcanism (Yin and Nie, 1996). The events were associated with subduction of Pacific and Philippine plates. These tectono-thermal events also resulted in replacement of the old, cold, thick, and depleted lithospheric mantle by young, hot, thin, and fertile lithospheric mantle accompanied by lithospheric thinning. Widespread Cenozoic rifting and associated alkaline basalt in the North China block are well documented. GPS measurements indicate that the South China block is moving southeastward at ~10 mm/year while the North China block is moving eastward at ~ 5 mm/year (Chen et al., 2000; Michel et al., 2000; Holt et al., 2000). The faster motion of the South China block produces shearing on the North China block. The Pn velocity image shows that low-velocity structures are NNE-elongate and correspond to a pattern of young volcanism and regions of large extension. The Shanxi rift, a continental rift located on the eastern edge of the Ordos Plateau, is characterized with low Pn velocity that mimics the en-echelon pattern of the right stepping Shanxi grabens. Beneath the Tai Shan, where the Tan Lu fault crosses, a very pronounced Pn velocity zone was imaged. The high elevation of this mountain region must be partially supported by the buoyant mantle, a cause that was not known before this study. The Hannuoba alkaline basalt that occurs north of Beijing and extends into Inner Mongolia is underlain by low Pn velocity. The overall low Pn velocity pattern and correlation with magmatism clearly demonstrate that the lithospheric mantle beneath the North China block is hot and partially melted. This interpretation is also consistent with the observed inefficient Sn propagation in this region (Rapine and Ni, 2001).

The interior of the North China block consists of the elevated Ordos plateau and the Yin Chuan rift located east of the Ordos plateau. Pn velocities beneath these regions are normal and indicate that Yin Chuan rift is a structural rift in an early stage of rifting and the thick crust there mostly supports the Ordos plateau.

The eastern part of South China block was a magmatic arc during much of the Mesozoic to Cenozoic. Low Pn velocity regions correlated well with region of Cenozoic magmatism. The ray coverage near Taiwan is poor and thus imaged features are not interpretable. A very low velocity feature is found north of Hainan Island in the Guangdong province. The close proximity of this feature to the Red River fault and South China Sea suggest a possible relationship between the opening of the South China Sea and the low Pn velocity feature.

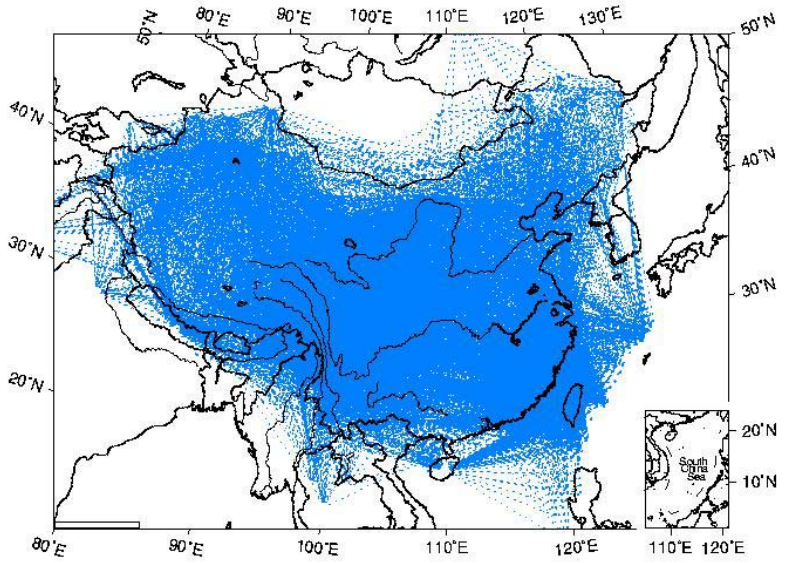

Figure 4. Pn raypaths used in the tomography. Distances were restricted to 1.8 to 15 degrees. About 25,000 raypaths are shown.

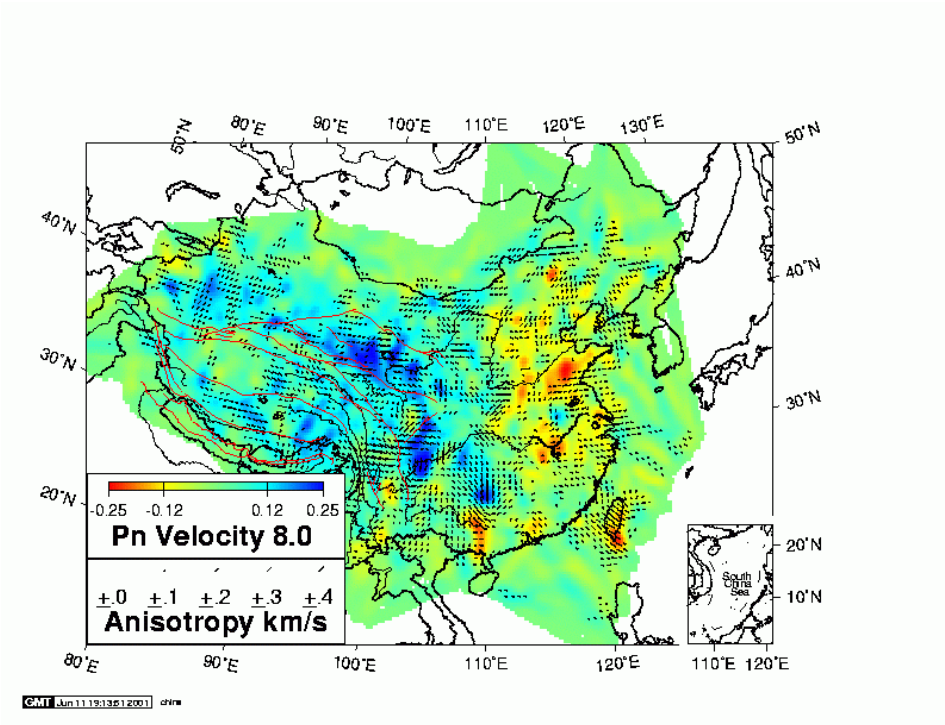

Figure 5. Pn velocity beneath China. Shades represent variations from a mean Pn velocity of 8.0 km/s. Line segments show the anisotropy with the line oriented in the fast direction. The Tarim, Tsidam, and western Sichaun basins have the highest Pn velocities. These places may be cratonic terrains that were accreted to southern Asia before the Indian-Asian collision. Eastern China has lower Pn velocities.

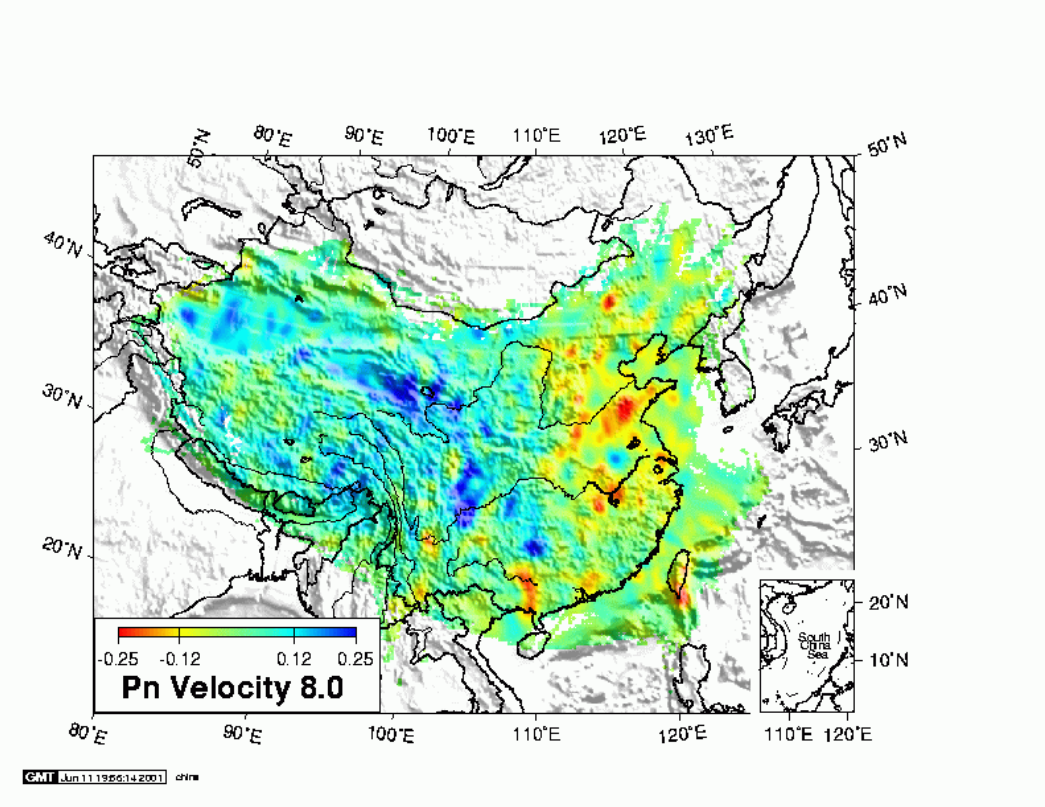

Figure 6. Pn velocity beneath China superimposed upon a shaded topographic relief map. Higher Pn velocities correspond to cratonic areas.

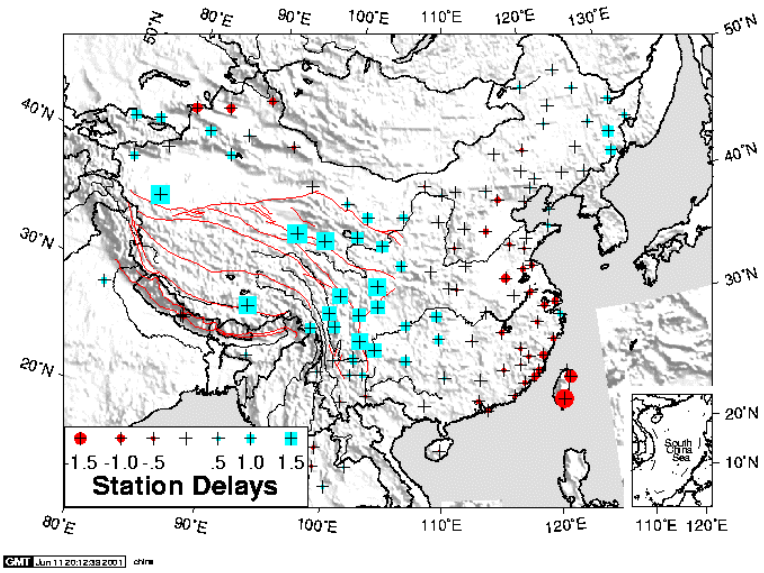

Figure 7. Station delays beneath China (zero-mean). These delays depend on both crustal thickness and crustal velocity. For a constant velocity crust, one second of delay corresponds to about 10 km of crustal thickening. Late arrivals in Lhasa, Tibet, and around the edges of the Tibetan Plateau result from the 70-km-thick crust. Early delays in the east and in Taiwan are the result of thinner crust.

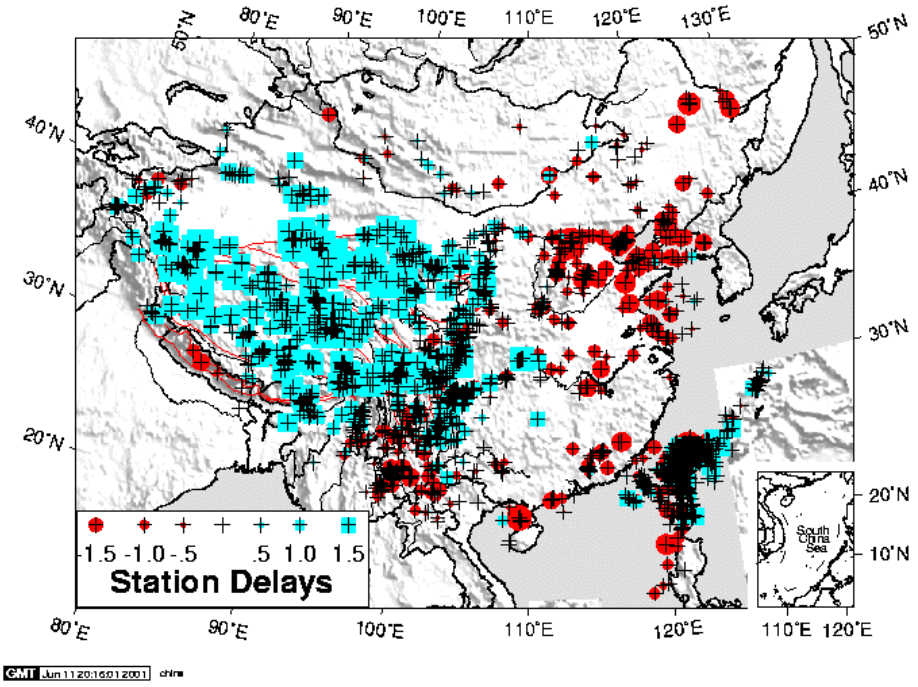

Figure 8. Event delays beneath China (zero-mean). Event delays also show the contrast between thick crust in the west and thin crust in the east.

CONCLUSIONS AND RECOMMENDATIONS

- The quality of the ABCE catalogs is excellent, with all seismic phases picked and identified on over 1030 stations. The consistency of the tomography event delays shows that the event locations are also of high quality and can be useful for CTBT station calibration purposes.
- Estimates of Pg, Pn, Sg, and Sn velocities as observed at 10 CDSN stations show little variation due to regional averaging. Pg velocities are typically 6.1 km/s; Pn velocities are 8.0 km/s; Sg velocities are 3.5 km/s; Sn velocities are 4.5 km/s.
- China shows a bimodal distribution of seismic velocity and crustal thickness. Western China, especially Tibet, has higher Pn velocities and thicker crust. High velocities generally represent older cratonic fragments, while lower velocities represent tectonically active regions. Variations in mantle velocity and crustal thickness beneath China will create bias in event locations unless corrected for.

REFERENCES

Akaike, H. (1992), Information theory and an extension of the maximum likelihood principle, in *Breakthroughs in Statistics, Vol. I, Foundations and Basic Theory*, S. Kotz and N.L. Johnson, eds, Springer-Verlag, New York, 610-624.

Annual Bulletin of Chinese Earthquakes (1982-1995), China Seismological Bureau.

Barazangi, M., and J. Ni, Velocities and propagation characteristics of Pn and Sn waves beneath the Himalayan Arc and Tibetan Plateau: Possible evidence for underthrusting of Indian continental lithosphere beneath Tibet, *Geology*, 10, 179-185, 1982.

Beghoul, N, M. Barazangi, B. Isacks (1993), Lithospheric structure of Tibet and Western North-America: Mechanisms of uplift and a comparative study, *J. Geophys. Res*, 98, 1997-2016.

Chen, W., B. Burchfiel, Y. Liu, R. King, L. Royden, W. tang, E. Wang, J. Zhao, and X. Zhang (2000), Global positioning system measurements from eastern Tibet and Their implications for India/Eurasia intercontinental deformation, *J. Geophys. Res.,* 105, 16215-16277.

Guzman-Speziale, M, and J. F. Ni (1993), The opening of the Andaman Sea: Where is the short-term displacement being taken up?, *Geophysical Research Letters*, 20, 2949 -2952.

Hearn, T. (1999), Uppermost mantle velocities and anisotropy beneath Europe, *J. Geophysical Research*, 104, 15,123-15,139.

Holt, W. (2000), Correlated crust and mantle strain fields in Tibet, *Geology*, 28, 67-70.

McNamara D.E., W. R. Walter, T. J. Owens, C. J. Ammon (1997), Upper mantle velocity structure beneath the Tibetan Plateau from Pn travel time tomography, J. Geophysical Research, 102, 493-505.

McQuarrie, A. and C-L Tsai (1998), *Regression and Time Series Model Selection*, World Scientific.

Michel, G., M. Becker, D. Anermann, C. Reigher, E. Reinhart and the GEOSSEA-Team (2001), New evidence for crustal motion in E and SE Asia from GPS measurements, *Earth Planet. Sci. Let*., 187, 239-244.

Nelson K.D., W. J.Zhao, L. D. Brown, J. Kuo, J. K. Che, X. W. Liu, S. L. Klemperer, Y. Makovsky, R. Meissner, J. Mechie, R. Kind, F. Wenzel, J. Ni, J. Nabelek, L. S. Chen, H. D. Tan, W. B. Wei, A. G. Jones, J. Booker, M. Unsworth, W. S. F. Kidd, M. Hauck, D. Alsdorf, A. Ross, M. Cogan, C. D. Wu, E. Sandvol, M. Edwards (1996), Partially molten middle crust beneath southern Tibet: Synthesis of project INDEPTH results *Science*, 274(#5293), 1684-1688.

Ni, J. and M. Barazangi (1983), Velocities and propagation characteristics of Pn, Pg, Sn, and Lg seismic waves beneath the Indian Shield, Himalayan Arc, Tibetan Plat eau, and surrounding regions: High uppermost mantle velocities and efficient Sn propagation beneath Tibet, *Geophys. J. R. Astr. Soc*. 72, 665-689.

Rapine, R. and J. Ni (2001), Propagation characteristics of Sn and Lg in northeastern China and Mongolia, *J. Geophys. Res.,* submitted.

Wei-Chuang H., J. F. Ni, F. Tilmann, D. Nelson, J. Guo, W. Zhao, J. Mechie, R. Kind, J. Saul, R. Rapine, and T. M. Hearn (2000), , Seismic polarization anisotropy beneath the central Tibetan Plateau, *Journal of Geophysical Research*, 105, 27979-27989.

Yin A, T. M. Harrison (2000), Geologic evolution of the Himalayan-Tibetan orogen, *Annual Review of Earth and Planetary Sciences*, 28, 211-280.

Yin, A. and S. A. Nei (1996), Phanerozoic palinspastic reconstruction of China and its neighboring regions, in *The Tectonic Evolution of Asia*, Cambridge University Press, 442-485.